Layered Copper Hydroxide *n*-Alkylsulfonate Salts: Synthesis, Characterization, and Magnetic Behaviors in Relation to the Basal Spacing

Seong-Hun Park[†] and Cheol Eui Lee*

Institute for Nano Science and Department of Physics, Korea University, Seoul 136-701, Korea

Received: July 13, 2004; In Final Form: October 11, 2004

A series of hybrid inorganic−organic copper(II) hydroxy *n*-alkylsulfonate with a triangular lattice, $Cu_2(OH)_3(C_nH_{2n+1}SO_3)$ ($n = 6, 8, 10$), are prepared by anion exchange, starting from copper hydroxy nitrate $Cu_2(OH)_3NO_3$. These compounds show a layered structure as determined by X-ray diffraction, with interlayer distances of 14.3−34.8 Å in alternation with interdigitated bilayer packing. Magnetic properties have been investigated by means of dc and ac measurements. All the compounds show similar metamagnet behaviors, with a Neel temperature of about 11 K. A subtle difference in the ac magnetic susceptibility among the compounds is understood by the existence of hydrogen bonding between the sulfonate headgroup and the hydroxide anion. A detailed molecular structure of the alkyl chains incorporated to the inorganic copper hydroxide layer is also discussed from the FTIR data.

1. Introduction

In recent years, inorganic−organic (I/O) materials[1] have been a subject of great attention because of the wide variations in the structures and molecular interactions and because of their extraordinary ability to combine synergistically the properties unique to purely organic or inorganic materials. Sustained interest in these materials can be attributed, in general, to a vast array of possibilities they offer in tailoring material properties simply by the correct selection of functionalized organics and variously coordinating inorganic precursors.[2] In particular, the field of inorganic−organic materials dominates the area of molecular magnets.[3]

The majority of these layered I/O materials are prepared by selective intercalation of organic moieties into a layered, inorganic host. Examples of this type include classes of materials obtained by intercalation of ionic/polymeric molecules through specific electrostatic or ionic interactions into layered host lattices of clays and silicates, double hydroxides, and metal phosphates and phosphonates.[4] In particular, there is considerable interest in anion-exchangeable layered compounds, which appear well-adapted to favor covalent links between the organic and inorganic constituents, because the anions are bonded to the metal ions and form the framework of the crystal, as in the case of the Botallackite-type layered compounds, $M_2(OH)_3X\cdot zH_2O$ (M^{II} = Co, Ni, and Cu; X = inorganic or organic anion).[5] These systems possess positively charged magnetic sheets formed by layered triangular networks of metal ions that are interleaved by an anion X^-. A remarkable feature of these series is that the intercalation of large organic species enables us to modulate the interlayer spacing over very large distances and hence to tune the magnetic properties depending on the interlayer separation.[6] Therefore, these systems appear appropriate for the design of I/O hybrid materials with outstanding magnetic properties.

Many efforts have been devoted in recent years to studying the role of the intercalated anions (carboxylate, dicarboxylate, and sulfate) on magnetic properties. In particular, the magnetic properties of materials involving copper(II) ions have been known to be very sensitive to any structural modification. For example, the *n*-alkyl carboxylate derivatives[7] with bilayer structures showed anomalous behaviors going from antiferromagnetic (AFM) to ferromagnetic (FM) states with varying layer spacing; in contrast, the analogous *n*-alkyl sulfate derivatives[8] with monolayer structures were all antiferromagnets. As a result, it is expected that large variations may be observed in the magnetic behavior of the exchanged compounds.

As regards the alkylsulfonate intercalated compounds, the examples are scarce in the literature. $M_2(OH)_3(C_{12}H_{25}SO_3)\cdot H_2O$ (M = Cu, Ni) and $Co_5(OH)_8(C_{12}H_{25}SO_3)_2\cdot 5H_2O$ are the only examples known so far.[9] The copper compounds exhibit a short-range antiferromagnetic interaction, whereas the nickel compounds are ferromagnets and the cobalt compounds are ferrimagnets. On the other hand, in our previous work, long-range magnetic order, with both antiferromagnetic and ferromagnetic interactions in copper-based alkylsulfonate anhydrates, has been observed.[10] To discuss the magnetic behavior of such compounds in relation to their dimensionality, a complete series of alkylsulfonate salts with different basal spacings is necessary.

In this extended work, we intend to report a detailed study for the synthesis of large molecular species based on sulfonate ligands and characterization of the chemical and magnetic properties of the series of layered copper(II) hydroxy salts, $Cu_2(OH)_3(C_nH_{2n+1}SO_3)$ with $n = 6$, 8, and 10 (denoted hereafter as CuLAS-*n*). In particular, it is necessary to understand the diverse magnetic properties of the copper-based hydroxide magnets $Cu_2(OH)_3X\cdot zH_2O$ with different anion functions in relation to the basal spacing and alkyl chain packing. The chain packing and conformation of the *n*-alkyl chains are discussed from a combined IR spectroscopy and X-ray diffraction study.

2. Experimental Section

2.1. Synthesis. A series of the copper(II) hydroxide-based system, CuLAS-*n*, were synthesized by an anionic exchange reaction starting from the layered copper(II) hydroxy nitrate

* Corresponding author. E-mail: rscel@korea.ac.kr.
[†] Present address: Nano Material Team, Korea Basic Science Institute (KBSI) at Daejeon.

10.1021/jp046902u CCC: $30.25
Published on Web 12/30/2004

$Cu_2(OH)_3NO_3$ (Cu-NO_3). The parent compound was obtained as in a previous report.[11] The anion exchange reaction used was very simple: the parent material (0.2 g) and the corresponding sodium *n*-alkanesulfonate (0.1 mol) were dispersed in distilled water. The mixture was stirred in an air-free round-bottomed flask for 48 h at room temperature. The shiny blue powder was then filtered, washed with distilled water and ethanol, and dried in a vacuum at 35 °C.

2.2. Characterization. Elemental analysis for carbon, nitrogen, hydrogen, and sulfur was performed at the Seoul Branch of Korea Basic Science Institute (KBSI). The powder X-ray diffraction data were collected on a MAC Science diffractometer (MXP3A-HF) operating at 40 kV and 30 mA in the Bragg−Brentano $\theta\angle 2\theta$ mode (Cu Kα1, 1.5424 Å). The X-ray measurements were done on naturally oriented samples on glass sample holders.

The FT-IR spectra were obtained using a FTIR Bomem Michelson spectrometer. Each sample was cast on a KBr pellet and measured in the transmission mode from 500 to 4000 cm^{-1} with a resolution of 4 cm^{-1}. The magnetic measurements on the powdered samples enclosed in a medical cap were carried out using a Quantum Design MPMS-7 SQUID magnetometer. The temperature dependence of the static susceptibility was examined in the range 5−300 K in a magnetic field of 5000 Oe. The hysteresis curves were obtained at 5 and 20 K in applied fields up to 7 T, after cooling with no applied field through the magnetic transitions. The ac susceptibility measurements were performed in a 1-Oe field in the frequency range 10−10 000 Hz, in the temperature range 5−30 K (PPMS, Quantum Design Co.).

3. Results and Discussion

3.1. Syntheses. While synthesis of the whole CuLAS-*n* ($n = 2-18$) series was attempted by means of anion exchanges, which was unsuccessful for CuLAS-2−4 and CuLAS-12−18 because of decomposition ($n = 2-4$) and incompleteness of the ion-exchange ($n = 12-18$). The latter may be due to the weak coordinating power of the sulfonate anion to the metal ion. As a result, only the CuLAS-*n* ($n = 6$, 8, and 10) compounds were obtained as polycrystals, whereas the CuLAS-4 and CuLAS-12 were obtained as mixed phases. Chemical analysis confirmed the composition of the CuLAS-*n* materials, indicating the total exchange of nitrate anions. [Anal. Calcd (found) for $C_6Cu_2H_{16}SO_6$ (CuLAS-6): C, 20.99 (21.03); H, 4.70 (4.86); N, 0.00 (0.07); S, 9.34 (8.20). Anal. Calcd (found) for $C_8Cu_2H_{20}SO_6$ (CuLAS-8): C, 25.87 (25.84); H, 5.43 (5.38); N, 0.00 (0.00); S, 8.63 (8.52). Anal. Calcd (found) for $C_{10}Cu_2H_{24}SO_6$ (CuLAS-10): C, 30.07 (29.92); H, 6.056 (6.033) N, 0.00 (0.00); S, 8.027 (8.124)]. For all compounds, it is noted that no lattice water is contained.

3.2. X-ray Powder Diffraction. As shown in Figure 1, the CuLAS-*n* compounds exhibit a lamellar structure as is evident from the powder XRD patterns exhibiting, in the low 2θ range, intense (00*l*) reflections, up to at least the third harmonic, corresponding to the stacking periodicity of the hydroxide-based layers. First of all, before extracting the crystallographic structure from the powder XRD patterns, it is necessary to confirm the completeness of the anion exchange reaction in the CuLAS-*n* series compounds, which can be checked simply via the relative changes in peak positions with respect to the starting material, $Cu_2(OH)_3NO_3$ ($d_{001} = 6.96$ Å). In all cases, since no reflections from the starting compound are observed, we can conclude that the total exchange reaction has been successfully realized. In addition, thanks to the high crystallinity of the samples, the

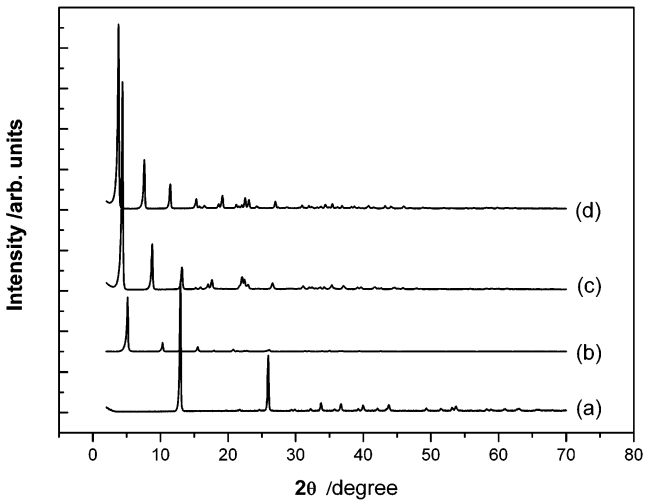

Figure 1. Powder X-ray diffraction patterns of (a) $Cu_2(OH)_3NO_3$ (parent compound) and (b−d) $Cu_2(OH)_3(C_nH_{2n+1}SO_3)$, where $n = 6$, 8, 10, respectively, showing the shift of 00*l* diffraction lines.

TABLE 1: Refined Cell Parameters and Basal Spacings for the CuLAS-*n*

sample	*a* (Å)	*b* (Å)	*c* (Å)	β (deg)	basal spacing (Å)
Cu-NO_3	5.598	6.085	6.930	94.75	6.96
CuLAS-6	5.588	6.074	17.813	106.03	17.1
CuLAS-8	5.591	6.065	21.614	111.53	20.1
CuLAS-10	5.599	6.050	25.268	114.04	23.3

X-ray diffraction data can be analyzed on the basis of a monoclinic structure, so that the resultant cell parameters can be compared with those of the parent material. The cell parameters were refined with sufficient precision using the "TREOR 90" indexing software and by profile (Pawley) refinement in Materials Studio v2.2 platform. As seen from Table 1, the cell parameters *a* and *b* for the intercalated compounds are very close to those reported for the monoclinic unit cell of the parent material, although the *c* parameter depends on the length of the alkyl chains.

It is well-known that the alkyl chain packing can be understood through an analysis of the variation in the fundamental layer spacing (d_{001}) with the alkyl chain length. As was established in a previous work, the basal spacing is related to the carbon chain length (*n*) through the relationship $d(\text{Å}) = d_0 + \eta(1.27n \cos\theta)$, where $\eta = 1$ or 2, depending on the chain packing and θ is the tilt angle of the chains.[12] In particular, the distance d_0 involves the size of the bridging group, the van der Waals distance between either facing methyl groups or methyl groups and hydroxide layers, and the thickness of the inorganic layer.

For the *n*-alkylsulfonate derivatives, as shown in Figure 2, the variation of the basal spacing increases linearly with the aliphatic chain length *n*, according to the relationship $d(\text{Å}) = 8.39 + 1.48n$. This indicates that, if the molecular area of the chains is constant, regardless of the *n* value, the *n*-alkyl chains are organized in a partially interdigitated bilayer packing with a tilt angle $\theta = 36°$, in very good agreement with previous findings for the Cu(II) parent compounds.[13] Tilt of the aliphatic chains or partial interdigitation of the chains results in a value between 1.27 and 2.52 Å/carbon atom. Using the same arguments, the intercept of the basal spacing vs the carbon chain length plot, d_0, can be assigned to the thickness of the inorganic layer (~3.0 Å) plus the surfactant headgroup (2.65 Å); $2.65 \times 2 + 3.0 = 8.3$ Å. This simple calculation agrees with the

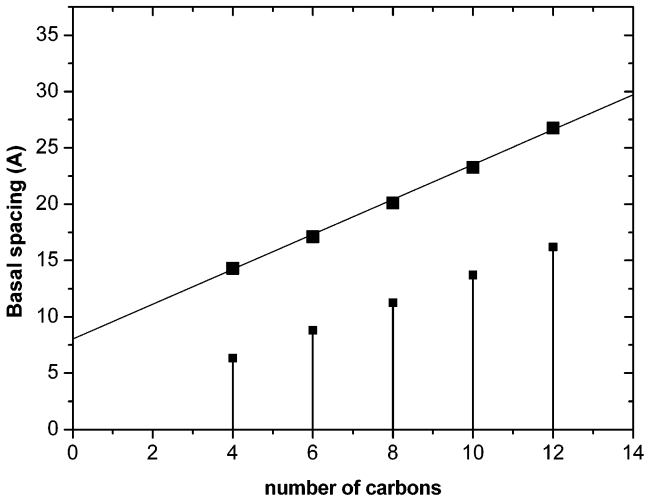

Figure 2. Dependence of the basal spacing on the carbon number in the copper(II) hydroxy *n*-alkylsulfonates. The vertical lines show the calculated molecular heights of sulfonates. Linear variations are observed. The values for CuLAS-4 and CuLAS-12 were obtained from structure analyses of the mixed phase samples obtained.

experimental value, 8.39 Å. From the resultant XRD data analyses, we are capable of extracting the lamellar structure for the CuLAS-*n* (n = 6, 8, and 10) as is displayed in Figure 3, consisting of alternating inorganic copper hydroxide layer and organic layers of aligned alkyl chains with partially interdigitated bilayer packing.

3.3. Infrared Study. IR spectroscopy has been known to be an effective technique capable of checking the completeness of the anion exchange reaction as well as understanding the molecular structure of the organic anions in the interlayer spaces.[14] For instance, from IR spectroscopy of alkyl chain assemblies such as *n*-alkylsulfonates, it is not difficult to extract some information on the metal−anion coordination, on the chain conformation, and on the packing of the alkyl chains even if the complete crystal structure is lacking. Indeed, IR spectroscopy is able to provide a firm basis of extension of the vibration analysis to related classes of chain assemblies including the organic−inorganic materials of concern here.

Fundamental Mode. The whole patterns of the characteristic IR spectra obtained are shown in Figure 4. For comparison, the IR spectrum of the parent material is also shown. The most distinct feature for the CuLAS-*n* and the parent material, Cu-NO_3, is noticed in two different wavenumber regions, i.e., 2900−3500 and 1000−1500 cm^{-1}, that correspond to the hydroxy groups and to the stretching vibrations of anions, respectively. In other words, the stretching vibration of the hydroxy groups is shifted to a lower frequency, which may be attributed to the weakness of O−H, and the weakness and/or absence of a broad feature in the hydrogen-bonding region (3550−3200 cm^{-1}) and the HOH bending mode (1630−1600 cm^{-1}). These features are indicative of no lattice water, in accordance with the elemental analysis. On the other hand, the disappearance of vibrations due to the N−O of the nitrate group, identified around 1423 cm^{-1}, and the appearance of the S−O band from the sulfonate group in the intercalated materials are observed. In effect, the IR spectra qualitatively confirm the total exchange of the nitrate by the sulfonate as well as the absence of lattice water.

Molecular Structure. To understand the molecular conformation or packing characteristics of the alkyl chains as well as the metal−anion coordination mode in the interlayer spaces, it is necessary to check the C−H vibration at high- and low-

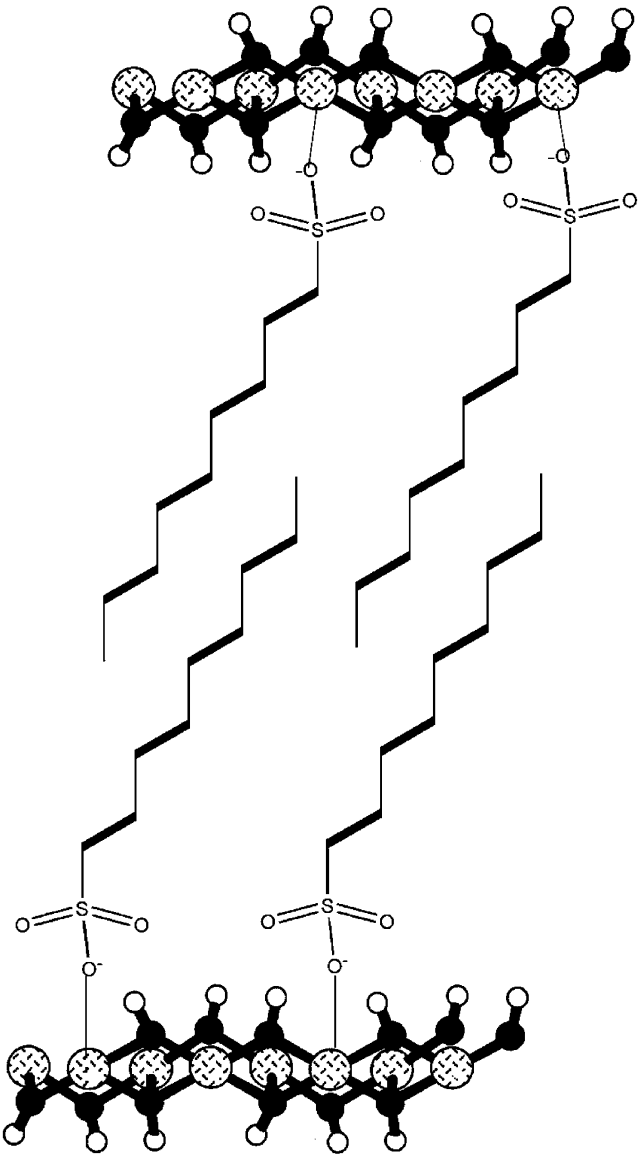

Figure 3. Model description of the proposed structure of the CuLAS-*n* (n = 6, 8, and 10). This structure is a modification of the botallackite ($Cu_2(OH)_3Cl$) type, where Cl ion is replaced with alkylsulfonate anion, consisting of alternating inorganic copper hydroxide layer and organic layers of aligned alkyl chains with partially interdigitated bilayer packing.

frequency regions in detail. In fact, the high-frequency region (2700−3100 cm^{-1}) reveals the C−H stretching modes of the methyl and the methylene groups while the low-frequency region of 600−1800 cm^{-1} displays the stretching modes of the sulfonate group as well as the scissoring, rocking, wagging, and twisting modes of the methylene groups (Figure 5).

The characteristic band-signatures (Figure 5) of overlapping peaks observed in the high-frequency region of the IR spectra are straightforwardly assigned to the C−H stretching modes of the polymethylene [$-(CH_2)_n-$] sequence and end-methyl ($-CH_3$) groups according to the previous assignments of the long-chain *n*-alkanes.[15] More specifically, the two intense bands at 2853−2851 and 2934−2919 cm^{-1} are assigned, respectively, to the symmetric ($\nu_s(CH_2),d^+$) and the antisymmetric ($\nu_{as}(CH_2),d^-$) stretching vibrations of the methylene groups. The peaks observed at 2872 and 2958 cm^{-1} are assigned to the symmetric ($\nu_s(CH_3),r^+$) and the antisymmetric ($\nu_{as}(CH_3),r^-$) stretching vibrations of the methyl groups, respectively. In the high-frequency region, two shoulder peaks are additionally identified

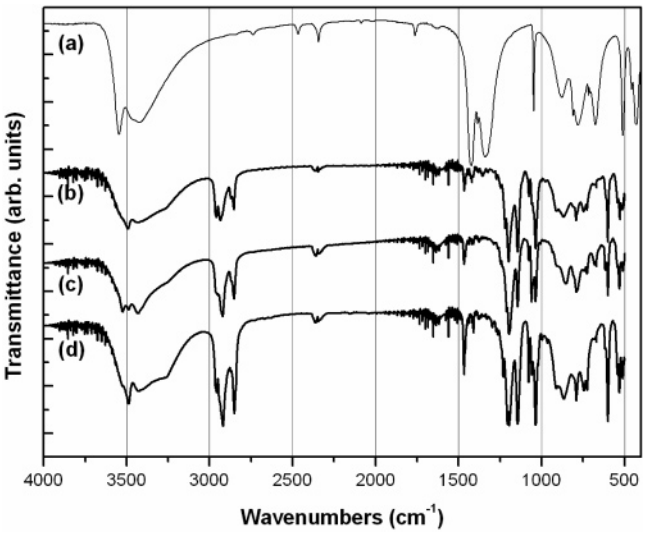

Figure 4. Infrared spectra for (a) $Cu_2(OH)_3NO_3$ (parent compound) and (b−d) $Cu_2(OH)_3(C_nH_{2n+1}SO_3)$, where $n = 6$, 8, 10, respectively.

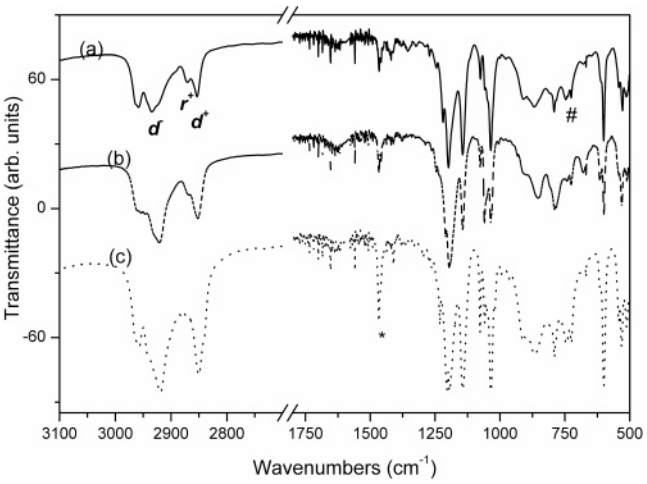

Figure 5. Infrared spectra of $Cu_2(OH)_3(C_nH_{2n+1}SO_3)$ where $n = 6$ (a), 8 (b), and 10 (c), respectively, in the high-frequency (2700−3100 cm^{-1}) region, showing overlapping contributions from CH_2 and CH_3 stretching modes (left), and in the lower frequency (500−1700 cm^{-1}) region, showing the stretching vibration of the sulfonate headgroup as well as the scissoring, rocking, wagging, and twisting modes of the methylene group.

at 2860 and 2965 cm^{-1}. The former peak can be attributed to the Fermi resonance absorption due to the d^+ mode, whereas the latter peak has to be attributed to the r^- mode. It is well-known that for the two antisymmetric stretching vibrations of a CH_3 group to become degenerate and appear as a single broad peak, the CH_3 group must be at least in a C_3 symmetry.[16] In the present case, the symmetry is apparently further lifted due to the interpenetration of the alkyl chains. The two antisymmetric vibrations will then no longer be equivalent, splitting into two peaks.

It has been well-established that the d^+ and d^- modes are strong indicators of the chain conformation. The d^+ and d^- modes usually lie in the narrow ranges of 2846−2850 and 2915−2918 cm^{-1}, respectively, for all-trans extended chains and in the distinctly different ranges of 2854−2856 and 2924−2928 cm^{-1} for disordered chains characterized by a significant presence of gauche conformers. On this basis, the observed peak frequencies of the d^+ and d^- modes suggest that the alkyl chains are in an all-trans conformational state with little or no significant gauche population.

The low-frequency region (650−1800 cm^{-1}) provides additional structural information regarding CuLAS-*n*. As mentioned previously, peaks appearing in this region are associated with the stretching vibration of the sulfonate group as well as with the scissoring, rocking, wagging, and twisting modes of the methylene group.

The three samples of CuLAS-*n* exhibit the characteristics of the fundamental and the split ν_3(S−O) stretching modes in the range of 1000−1250 cm^{-1}. Two stretching vibrations of SO_3, i.e., $\nu_{as}(SO_3^-)$ and $\nu_s(SO_3^-)$, are observed at 1195−1198 and 1035 cm^{-1}, respectively, whereas in free ligands the two bands appear at 1175 and 1050 cm^{-1}, respectively. Furthermore, the difference $\Delta\nu$ ($=\nu_{as} - \nu_s$) obtained here is ca. 160 cm^{-1}, which is greater than that of the ligand ($\Delta\nu = 125$ cm^{-1}), as expected for the unidentate SO_3 coordination, and is very close to that reported by Kurmoo et al. for the isotypic compound $Ni_2(OH)_3(C_{12}H_{25}SO_3)\cdot H_2O$.[9]

The appearance of a single narrow peak at 1473 or 1467 cm^{-1} has been attributed to triclinic or hexagonal subcell packing, respectively. The appearance of a well-resolved doublet with two distinct components is known to occur either as a result of the intermolecular vibrational coupling due to a crystal-field splitting in the orthorhombic or monoclinic packing or as a result of the coexistence of triclinic and hexagonal packing in the material.[17] In addition, the peak is known to be broad when the alkyl chains assume a disordered conformation. On these grounds, the fact that a well-resolved doublet band is observed at 1467 cm^{-1} suggests a hexagonal packing with disordered conformation of all-trans chains.

The IR and X-ray diffraction studies show that the structural features of the CuLAS-*n* arise mainly from the amphiphilic nature of the intercalated alkylsulfonate anions in two ways: (i) the hydrophobic alkyl chain enables the layers to be spaced up to 23.3 Å apart, being tightly packed with hexagonal subcells between the layers, and (ii) the hydrophilic sulfonate headgroups are directly bonded to copper(II) ions, leading to partial interdigitated bilayer packing between the inorganic layers.

3.4. Magnetic Properties. The magnetic properties of materials involving copper(II) ions are known to be very sensitive to any structural modification that may be introduced by sulfate or carboxylate bridging species. A remarkable feature of those systems is that the magnetic properties and the stoichiometries, determined by the lattice water contents, are strongly correlated. It has been known that both *n*-alkyl sulfate and carboxylate derivatives with long chains have two different structural varieties. In particular, for the carboxylate derivatives, the hydrous α-phase is AFM, but the anhydrous β-phase is FM. Thus, great variations should be observed in the magnetic behaviors of the exchanged compounds depending on the water contents as well as the alkyl chain packing.

Our preceding work showed that the newly synthesized copper-based alkylsulfonate anhydrous compounds possess a long-range order,[10] in contrast to the hydrated derivatives exhibiting no sign of long-range order. To see the effect of molecular size of the intercalated anion on the magnetic behavior of the inorganic layer, we have carried out magnetic measurements on the new series of alkylsulfonate derivatives with no lattice water.

The magnetic susceptibility data were recorded for all CuLAS-*n* from 5 K to room temperature with $H_{dc} = 0.5$ T. The temperature dependences of χ and the χT product for CuLAS-*n* are plotted in Figures 6−8. All the compounds exhibit a similar magnetic behavior. At high temperatures, the χT values correspond to two Cu(II) (d^9, $S = 1/2$) per mole (ca. 0.8 emu

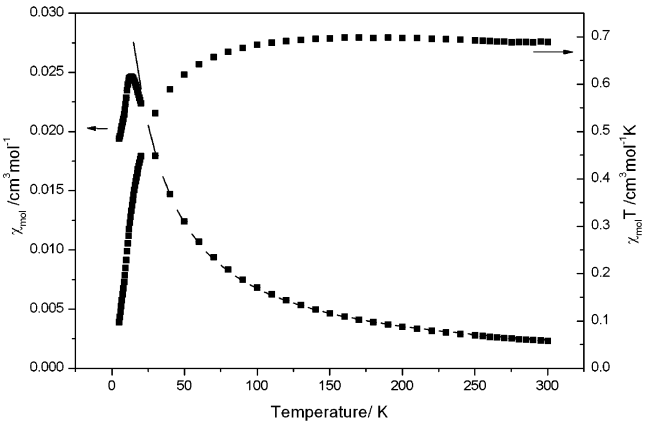

Figure 6. The temperature dependence of χ and the χT product for CuLAS-6. The solid line indicates a high-temperature fit to the 2D Heisenberg model.

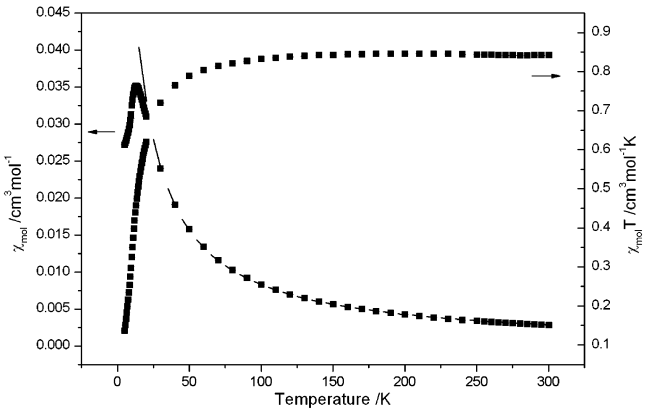

Figure 7. The temperature dependence of χ and the χT product for CuLAS-8. The solid line indicates a high-temperature fit to the 2D Heisenberg model.

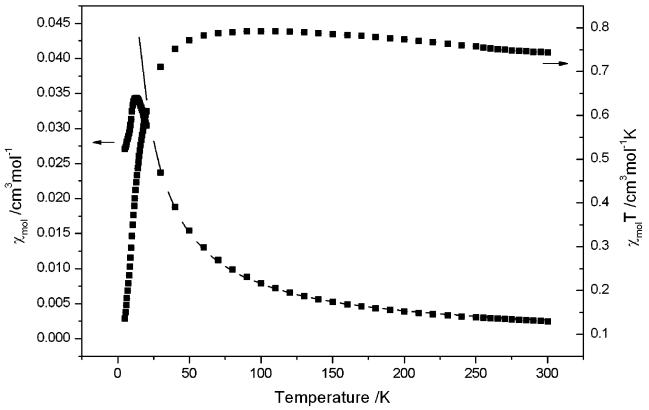

Figure 8. The temperature dependence of χ and the χT product for CuLAS-10. The solid line indicates a high-temperature fit to the 2D Heisenberg model.

kmol^{-1}). The values of χT for CuLAS-*n* at high temperatures increase with decreasing temperature, indicative of a ferromagnetic interaction. However, the marked decreases in χT at low temperatures are indicative of an interlayer antiferromagnetic coupling.[18] The magnetic data above 150 K can be fitted well to the Curie−Weiss law with $C = 0.668$ cm^3 mol^{-1} K and $\Theta = 8.54$ K ($n = 6$), $C = 0.833$ cm^3 mol^{-1} K and $\Theta = 3.04$ K ($n = 8$), and $C = 0.689$ cm^3 mol^{-1} K and $\Theta = 22.1$ K ($n = 10$). A fit of the magnetic susceptibility was made in the paramagnetic regime to determine the in-plane exchange interaction between the copper(II) ions. Using the high-temperature series expansions for the spin 1/2 2D Heisenberg triangular lattice,[19] a very good agreement between theory and experimental findings was obtained with $J/k = 2.725$, 0.38, and 10.8 K for $n = 6$, 8, and 10, respectively. A summary of the main magnetic results is given in Table 2.

TABLE 2: Main Magnetic Results

sample	basal spacing (Å)	T_N/K[a]	Θ/K[b]	C/cm^3 mol^{-1} K[b]
CuLAS-6	17.1	11.5	8.54	0.668
CuLAS-8	20.1	10.2	3.04	0.833
CuLAS-10	23.3	11.0	22.1	0.689

[a] The Neel temperature, T_N, was determined from the sharp peak in the ac magnetic susceptibility. [b] The Θ values were obtained from the high-temperature fit of the dc magnetic susceptibility, $\chi^{-1} = (T - \Theta)/C$.

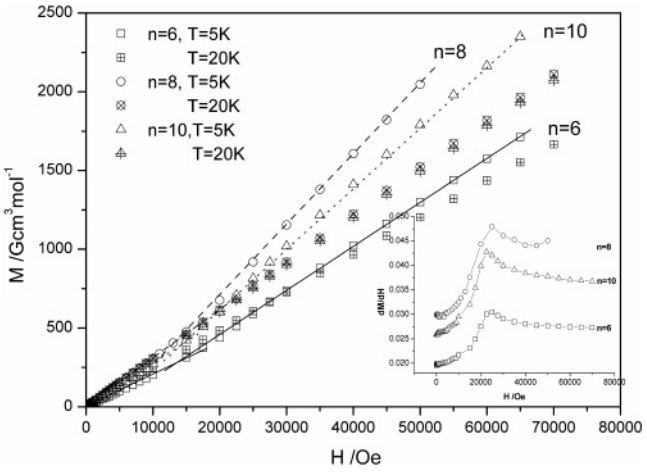

Figure 9. Magnetic field dependence of the magnetization of $Cu_2(OH)_3(C_nH_{2n+1}SO_3)$ at 5 K (below) and 20 K (above T_N), for $n = 6$, 8, and 10. Inset: the derivative of the field dependence, clearly showing a discontinuity behavior.

As shown in Figure 9, the field dependences of the magnetization below T_N (at 5 K) also show a pronounced sigmoidal shape with an inflection point at a critical field of about 2.5 T and with an increase in the slope at higher fields, which is attributed to a spin−flop transition. This is consistent with the coexistence of the ferromagnetic and antiferromagnetic interactions, which is characteristic of a metamagnet. The observed behaviors are similar to those of the transition metal hydroxides $M(OH)_2$, with M = Fe, Co, and Ni, which are well-characterized as metamagnets.[20]

Further information on the three-dimensional ordering is provided by the temperature dependence of the ac magnetic susceptibility, in a magnetic field $H_{ac} = 1$ Oe and at the ac frequency of 10 kHz (Figure 10). The in-phase χ'_{ac} of the ac susceptibility for all the samples increase with decreasing temperature, with a rather broad maximum at around 13 K, which is expected for a two-dimensional antiferromagnet. No frequency-dependent behavior was observed. While all the samples exhibit a broad maximum at around 13 K, apparently distinct behaviors are noticed between the CuLAS-6, -10 and CuLAS-8 materials. Specifically, while a pronounced sharp peak is observed for CuLAS-6 and CuLAS-10, it appears that the sharp peak is much suppressed for the CuLAS-8, leaving only a sign of the anomalous behavior. The sharp peaks in both χ'_{ac} and χ''_{ac} are taken to be indicative of a FM order, expected for a metamagnet built of spin-canted antiferromagnetic layers. The Neel temperature, T_N, of the CuLAS-*n* ($n = 6$, 8, and 10)

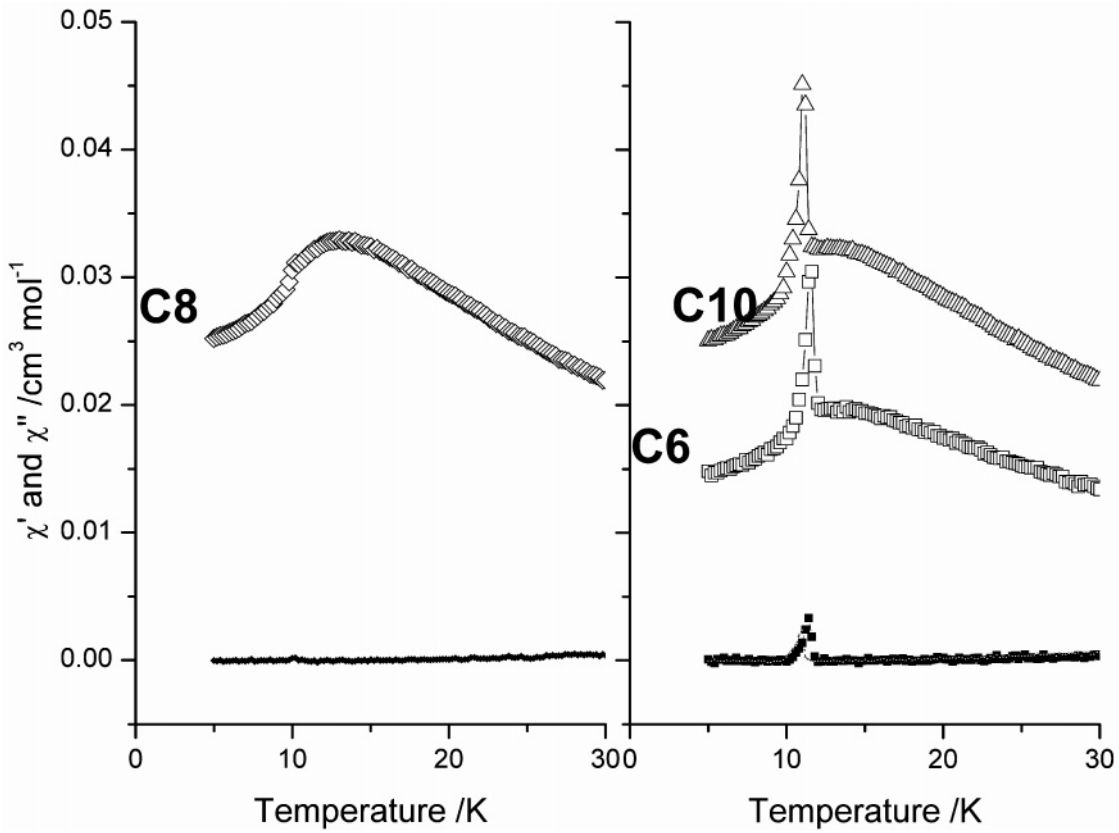

Figure 10. The temperature dependence of the ac susceptibility of $Cu_2(OH)_3(C_nH_{2n+1}SO_3)$.

material was determined to be 11.5, 10.2, and 11.0 K, respectively, from the sharp peaks in the ac magnetic susceptibilities.

It is worth noting that long-range magnetic behavior is observed with the interlayer distance up to 23.3 Å, in contrast to the hydrated copper(II) alkylsulfonate derivatives exhibiting no sign of a long-range order. While all the compounds exhibit similar magnetic behaviors, as shown in Table 2, it is worthwhile to discuss the origin of the distinct magnetic behaviors of the CuLAS-8 versus the CuLAS-6, 10 materials; The CuLAS-8 material shows a higher Curie constant and a lower Weiss temperature as well as the suppressed low-temperature sharp peak in the ac magnetic susceptibility. A small difference in the alkyl chain lengths in the compounds may give rise to slight in-plane structural modifications and thus to different exchange interactions. In fact, a careful inspection of the IR spectra (Figure 4) reveals subtle differences between the compounds in the characteristic frequency regions, i.e., hydrogen bonding (3200−3550 cm^{-1}) and sulfonate group regions (1000−1250 cm^{-1}), indicating the existence of hydrogen bonding between an oxygen in the SO_3 headgroup and the OH in the copper hydroxide layer.

Drillon and Panissod[21] have proposed a model to explain the magnetic behavior of layered compounds in relation to the basal spacing. In this model, for the in-plane ferromagnetic interactions, the in-plane spin moments align within the correlation domains whose sizes increase upon cooling, thus leading to giant magnetic moments in each layer. The interaction between these moments depends on the interlayer distance. For small distances, superexchange interaction occurs via hydrogen bonds and may lead to antiferromagnetic or metamagnetic order. In turn, for large distances, the through-space dipole−dipole interaction between the layers becomes predominant and favors long-range ferromagnetic order. In the present system, although the magnetic layers are well-separated with large distances, the existence of hydrogen bonding may block a 3D long-range order between the layers, resulting in the much suppressed sharp peaks indicative of the 3D order as is observed in our ac magnetic susceptibility measurements.

4. Conclusions

A novel series of layered copper hydroxide-based sulfonate compounds, CuLAS-*n* (n = 6, 8, 10), has been prepared by exchange reaction starting from the corresponding layered copper hydroxy nitrate. X-ray powder diffraction investigations show that these materials derive from the brucite structure by replacing nitrate groups by sulfonates and that alkyl chains are interleaved with partially interdigitated bilayer packing between the copper hydroxide layers. According to the FTIR study, the alkylsulfonates are completely exchanged and bonded to the metal via a unidentate binding mode. The magnetic properties have been investigated and explained by taking into account the main structural features evidenced by XRD and IR studies. These anhydrous materials exhibit a long-range magnetic order, while the hydrated derivatives show no sign of a long-range order. The CuLAS-*n* series show a similar metamagnet behavior at lower temperatures, with $T_N \sim 11$ K, corresponding to the presence of ferromagnetic subnetworks weakly coupled by antiferromagnetic coupling. The different behaviors are understood by the existence of hydrogen bonding, giving rise to slight in-plane structural modifications and thus to exchange interactions.

Acknowledgment. This work was supported by the KISTEP (National Research Laboratory and M102KS010001-02K1901-01814) and by the Korea Research Foundation (Brain Korea Project in 2004 and Grant No. KRF-2004-005-00060). Measurements at the Seoul Branch of the Korea Basic Science of Institute (KBSI) are gratefully acknowledged.

References and Notes

(1) (a) Levy, F. *Intercalated Layered Materials*; D. Reidel: Dordrecht, The Netherlands, 1979. (b) Wittingham, M. S.; Jacobson, R. A. *Intercalation Chemistry*; Academic: New York, 1982. (c) Giannelis, E. P. *Adv. Mater*. **1996**, *8*, 26. (d) Fergusson, G. S.; Kleinfeld, E. R. *Adv. Mater*. **1995**, *7*, 414. (e) Alberti, G.; Marmottini, F.; Murciamascaros, S.; Vivani, R. *Angew. Chem., Int. Ed. Engl*. **1994**, *33*, 15. (f) Alberti, G.; Casciola, M.; Constantino, U.; Vivani, R. *Adv. Mater*. **1996**, *8*, 291. (g) Novak, B. M. *Adv. Mater*. **1993**, *5*, 422.

(2) (a) Desiraju, G. *Crystal Engineering the Design of Organic Solids*; Elsevier: New York, 1989. (b) Stein, A.; Keller, S. W.; Mallouk, T. E. *Science* **1993**, *259*, 1558, and references therein.

(3) (a) Day, P. *J. Chem. Soc., Dalton Trans*. **1997**, 701. (b) Mitzi, D. B. *Prog. Inorg. Chem*. **1999**, *48*, 1. (c) Coronado, E.; Galán-Mascarós, J.-R.; Gómez-García, C. J.; Laukin, V. *Nature* **2000**, *408*, 447. (d) Clearfield, A. *Prog. Inorg. Chem*. **1998**, *47*, 371. (e) Tolbert, S. H.; Sieger, P.; Stucky, G. D.; Aubin, S. M. J.; Wu, C.-C.; Hendrickson, D. N. *J. Am. Chem. Soc*. **1997**, *119*, 8652. (f) Carling, S. G.; Mathonière, C.; Day, P.; Malik, K. M. A.; Coles, S. J.; Hursthouse, M. B. *J. Chem. Soc., Dalton Trans*. **1996**, 1839.

(4) O'Hare, D. *New J. Chem*. **1994**, *18*, 989, and selected references therein.

(5) (a) Miyata, S.; Kumura, T. *Chem. Lett.* **1973**, 843. (b) Yamanaka, S.; Sato, T.; Hattori, M. *Chem. Lett*. **1989**, 1869. (c) Yamanaka, S.; Sato, T.; Seki, K.; Hattori, M. *Solid State Ionics* **1992**, *53*−*56*, 527. (d) Rabu, P.; Angelov, S.; Legoll, P.; Belaiche, M.; Drillon, M. *Inorg. Chem.* **1993**, *32*, 2463. (e) Rouba, S.; Rabu, P.; Ressouche, E.; Regnault, L.-P.; Drillon, M. *J. Magn. Magn. Mater*. **1996**, *163*, 365.

(6) (a) Rabu, P.; Drillon, M. *Adv. Eng. Mater*. **2003**, *5*, 189. (b) Rabu, P.; Drillon, M.; Hornick, C. *Analysis* **2000**, *28*, 103. (c) Laget, V.; Hornick, C.; Rabu, P.; Drillon, M.; Ziessel, R. *Coord. Chem. Rev.* **1998**, *178*−*180*, 1533. (d) Fujita, W.; Awaga, K.; Yokoyama, T. *Appl. Clay Sci*. **1999**, *15*, 281.

(7) (a) Rabu, P.; Rouba, S.; Laget, V.; Hornick, C.; Drillon, M. *J. Chem. Soc., Chem. Commun*. **1996**, 1107. (b) Laget, V.; Drillon, M.; Hornick, C.; Trabu, P.; Romero, F.; Turek, P.; Ziessel, R. *J. Alloys Compds.* **1997**, *262*−*263*, 423. (c) Laget, V.; Hornick, C.; Rabu, P.; Drillon, M. *J. Mater. Chem*. **1999**, *9*, 169. (d) Fujita, W.; Awaga, K. *Inorg. Chem*. **1996**, *35*, 1915. (b) Fujita, W.; Awaga, K.; Yokoyama, T. *Inorg. Chem*. **1997**, *36*, 196.

(8) (a) Laget, V.; Rouba, S.; Hornick, C.; Drillon, M. *J. Magn. Magn. Mater*. **1996**, *154*, L7. (b) Okazaki, M.; Toriyama, K.; Tomura, S.; Kodama, T.; Watanabe, E. *Inorg. Chem*. **2000**, *39*, 2855.

(9) Kurmoo, M.; Day, P.; Derory, A.; Estoures, C.; Poinsot, R.; Stead, M. J.; Kepert, C. J. *J. Sol. State Chem.* **1999**, *145*, 452.

(10) Park, S.-H.; Lee, C. H.; Lee, C. E.; Ri, H.-C.; Shim. S. Y. *Mater. Res. Bull.* **2002**, *37*, 1773.

(11) Meyn, M.; Beneke, K.; Lagaly, G. *Inorg. Chem*. **1993**, *32*, 1209.

(12) Kitaigorodskii, A. I. *Organic Chemical Crystallography*; Consultants Bureau: New York, 1955.

(13) Rabu, P.; Drillon, M.; Awaga, K.; Fujita, W.; Sekine, T. In *Magnetism: Molecules to Materials II*; Miller, J. S., Drillon, M., Eds.; Wiley VCH: Weinheim, 2001, 357.

(14) (a) Nakamoto, K. *Infrared and Raman Spectra of Inorganic and Coordination Compounds*, 5th ed.; John Wiley & Sons: New York, 1997. (b) Colthup, N. B. *Introduction to Infrared and Raman Spectroscopy*, 3rd ed.; Academic Press: New York, 1990.

(15) (a) Wallach, D. F. H.; Verma, S. P.; Fookson, J. *Biochim. Biophys. Acta* **1979**, *559*, 153. (b) Snyder, R. G.; Schachtschnelder, J. H. *Spectrochim. Acta* **1963**, *19*, 85. (c) Tasumi, M.; Shimaanouchi, T.; Watanabe, A.; Goto, R. *Spectrochim. Acta* **1964**, *20*, 629. (d) Nuzzo, R. G.; Korenic, E. M.; Dubois, L. H. *J. Chem. Phys*. **1990**, *93*, 767.

(16) (a) Snyder, R. G.; Strauss, H. L.; Elliger, C. A. *J. Phys. Chem*. **1982**, *86*, 5145. (b) Snyder, R. G.; Maroncelli, M.; Strauss, H. L.; Hallmark, V. M. *J. Phys. Chem*. **1986**, *90*, 5623. (c) MacPhail, R. A.; Snyder, R. G.; Strauss, H. L. *J. Chem. Phys*. **1982**, *77*, 1118.

(17) (a) Borja, M.; Dutta, P. K. *J. Phys. Chem*. **1992**, *96*, 5434. (b) Almirante, C.; Minoni, G.; Zerbi, G. *J. Phys. Chem*. **1986**, *90*, 852.

(18) Carlin, R. L. *Magnetochemistry*; Springer-Verlag: Berlin, 1986; p122.

(19) Elstner, N.; Singh, R. R. P.; Young, A. P. *Phys. Rev. Lett*. **1993**, *71*, 1629.

(20) (a) Takada, T.; Bando, Y.; Kiyama, M.; Miyamoto, H. *J. Phys. Soc. Jpn.* **1966**, *21*, 2726. (b) Takada, T.; Bando, Y.; Kiyama, M.; Miyamoto, H. *J. Phys. Soc. Jpn*. **1966**, *21*, 2745. (c) Miyamoto, H.; Shinjo, T.; Bando, Y.; Takada, T. *J. Phys. Soc. Jpn*. **1967**, *23*, 1421.

(21) Drillon, M.; Panissod, P. *J. Magn. Magn. Mater*. **1998**, *188*, 93.